The use of ATSR active fire counts for estimating relative patterns of biomass burning – a study from the boreal forest region

Eric S. Kasischke
Department of Geography, University of Maryland, College Park, Maryland, USA

Jennifer H. Hewson
Department of Geography, University of Maryland, College Park, Maryland, USA

Brian Stocks
Canadian Forest Service, Sault Ste. Marie, Ontario, Canada

Guido van der Werf
USDA-FAS, NASA Goddard Space Flight Center, Greenbelt, Maryland, USA

James Randerson
Divisions of Geological and Planetary Sciences and Engineering and Applied Science, California Institute of Technology, Pasadena, California, USA

Received 29 May 2003; revised 19 August 2003; accepted 26 August 2003; published 30 September 2003.

[1] Satellite fire products have the potential to construct inter-annual time series of fire activity, but estimating area burned requires considering biases introduced by orbiting geometry, fire behavior, and the presence of clouds and smoke. Here we evaluated the performance of fire counts from the Advanced Thermal Scanning Radiometer (ATSR) for the boreal forest region using area burned information from other sources. We found ATSR detection rate varied between regions and different years, being higher during large fire years than during small fire years. The results show ATSR fire counts do not represent an unbiased sample of fire activity, and independent validation may be required prior to using this data set in studies of global emissions from biomass burning. *INDEX TERMS:* 0305 Atmospheric Composition and Structure: Aerosols and particles (0345, 4801); 0315 Atmospheric Composition and Structure: Biosphere/atmosphere interactions; 0933 Exploration Geophysics: Remote sensing. **Citation:** Kasischke, E. S., J. H. Hewson, B. Stocks, G. van der Werf, and J. Randerson, The use of ATSR active fire counts for estimating relative patterns of biomass burning – a study from the boreal forest region, *Geophys. Res. Lett.*, *30*(18), 1969, doi:10.1029/2003GL017859, 2003.

1. Introduction

[2] Wildland fire and vegetation burning are important processes in a number of biomes [*Goldammer*, 1990; *Kasischke and Stocks*, 2000; *Moreno and Oechel*, 1994], and a large and variable source of trace gas and particulate emissions [*Bergamaschi et al.*, 2000; *Hao and Ward*, 1993; *Lavoue et al.*, 2000; *van der Werf et al.*, 2003]. Studies of fire impacts over large areas and long time periods have been limited by the lack of quantitative information. Even though burned area statistics and databases have been compiled at national scales in some regions [*FAO*, 1999; *Stocks et al.*, 2003], reliable data sources do not exist for many areas, particularly Africa, South America, Asia, and Russia.

[3] Interest in using satellite remote sensing systems to monitor biomass burning began when *Dozier* [1981] found small, sub-pixel-sized fires could be detected using moderate resolution (~1 km), thermal infrared (IR) sensors. Subsequently, methods were developed to generate active fire products using data from the Advanced Very High Resolution Radiometer (AVHRR) [*Stroppiana et al.*, 2000], the ATSR [*Arino et al.*, 2001], the Visible and Infrared Scanner (VIRS) [*Giglio et al.*, 2000], and the Moderate Resolution Imaging Spectrometer (MODIS) [*Justice et al.*, 2002]. Assuming these data represent an unbiased sample of fire activity and indicate relative area burned between regions and years, AVHRR data have been used have been used to analyze the global distribution of fires [*Dwyer et al.*, 1998], and ATSR data have been used to scale biomass burning emissions between regions and years [*Schultz*, 2002; *Duncan et al.*, 2003]. Only in a few cases were efforts taken to independently calibrate the active fire count products through direct comparison to burned area information [*Eva and Lambin*, 1998; *Scholes et al.*, 1996; *Fuller and Folk*, 2001; *van der Werf et al.*, 2003].

2. Methods

[4] We evaluated the assumption that satellite-derived active fire products from ATSR (the World Fire Atlas Product–WFAP) represent an unbiased sample of fire activity by analyzing data from the boreal forest region. The WFAP dataset used (January 1997 to October 2002) was produced from two algorithms applied to nighttime data from the ATSR's thermal IR channel (3.7 μm): Algorithm 1 (WFAP-1) uses a threshold of 312 K and Algorithm 2 (WFAP-2) a threshold of 308 K. Three area burned data sets were used: (a) boundaries of large fire events >400 ha in size in 1997 in Alaska and Canada [*Kasischke et al.*, 2002; *Stocks et al.*, 2003]; (b) boundaries of large fires

0094-8276/03/2003GL017859

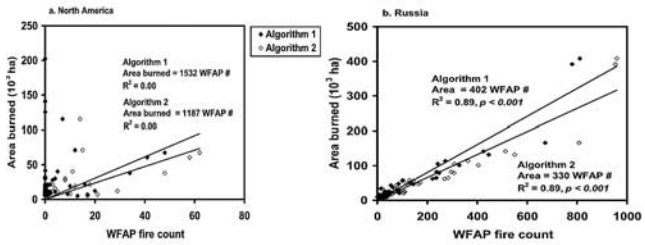

Figure 1. Area burned within specific fire events as a function of WFAP fire count. (a) Canada and Alaska in 1997; (b) Khabarovsk, Russia in 1998 (In this region, no fires were within 5 km of one another, and the buffering process did not result in the merging of any fire event.)

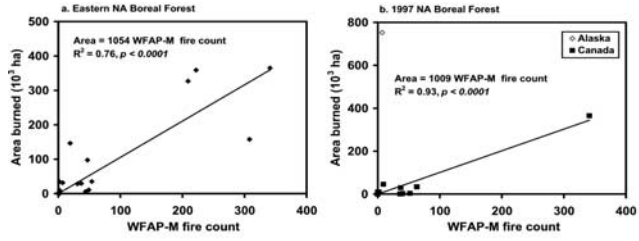

Figure 2. Area burned in different states, provinces and territories of Canada and Alaska as a function of WFAP fire count. (a) for East Canada; and (b) for the year 1997 (the same trend was observed using the WFAP-1 and WFAP-2 data).

in Khabarovsk, Russia in 1998 mapped from SPOT VEGETATION imagery; and (c) area burned statistics in Canada and Alaska compiled by fire management agencies for 1997 to 2002. Reliable data are available for Canada and Alaska because fire management agencies use aerial surveillance capabilities and all substantial fires are mapped. Since the early 1990s, global positioning systems have been used to insure accurate of fire perimeter locations. For the 1997 fire boundaries, a 1 km buffer was added to allow for uncertainties in the ATSR sensor.

[5] SPOT VEGETATION data [10-day Global Synthesis (VGT-S10) produced by the Flemish Institute for Technological Research] were used to map fire perimeters for the northeastern part of Khabarovsk, Russia in 1998. Using VGT-S10 images, the perimeters were manually outlined for 43 fire events (6,000 to 400,000 ha), and their accuracy checked through comparisons with quick-look Landsat ETM imagery. In comparing the boundaries of fires derived from the VGT-S10 imagery to WFAP fire detections, a 1.8 km buffer was added to allow for uncertainties associated with the spatial accuracy of the SPOT VEGETATION (0.8 km) and the ATSR sensors (1.0 km).

3. Results

[6] In 1997, 533 fire counts were detected by the WFAP-1 and 820 counts by the WFAP-2. Of these, 265 WFAP-1 counts and 368 WFAP-2 counts corresponded to actual fire events; thus, the false alarm rate is 50% at best for the standard WFAP products (Table 1). No fires smaller than 2,500 ha were detected, with the rate of detection increasing with fire size. For fires >2,500 ha, the WFAP algorithms detected 27 to 32% of all fires. Because of the low detection rate of individual fires, there was no significant linear correlation between fire count and actual area burned (Figure 1a). Figure 1b shows area burned (from VGT-S10 imagery) as a function of WFAP fire count in Khabarovsk in 1998. While the rate of detection of fires >300,000 ha is lower than for smaller fires, the WFAP fire count accounts for 89% of the variation in area burned in Khabarovsk, and all fires corresponded with a mapped fire perimeter (no false alarms).

[7] A question arising from Figure 1 is why did the ATSR exhibit poor detection for fires in North America in 1997? Most of the 1997 North American area burned occurred in fires in Interior Alaska, a region at a latitude >65° N where the local time for sunset is after midnight in mid-summer. Since the overpass time of the ATSR sensor is ~10 p.m. local, it does not always view fires at night, which impedes detection and may introduce false alarms. To address this issue, we filtered the WFAP-1 product to remove cases where collection occurred while sunlight was present, and where hotspots were detected 8 months out of the year. This process (WFAP-M) eliminated 89% of the hotspots in Alaska, 14% in the Northwest Territories, 12% in Ontario, and 2% in the Yukon Territories.

[8] For East Canada (provinces east of and including Ontario), a linear trend existed between area burned in individual provinces and territories for all years as a function of WFAP-M fire count (Figure 2a). This trend also existed for West/Central Canada (Saskatchewan, Manitoba, Alberta, British Columbia), and Northern Canada (Alaska, Northwest/Yukon Territories) (Table 2); however, the detection rate (slope of the regression line) was half as great in East Canada as in the other regions. Figure 2b presents a plot of area burned in the individual provinces and territories as a function of WFAP-M fire count during 1997. Linear regressions for the different years were calculated without Alaska because of the biases in this region.

Table 1. Summary of Fires During 1997 in Canada and Alaska Detected by the WFAP Active Fire Counts and Percent of Annual Area Burned as a Function of Fire Size for Small and Large Fire Years (after *Kasischke et al.*, 2002)

		Fires Detected		Rate of Detection		Percent of total area burned	
Fire size (10^3 ha)	Total fires	WFAP-1	WFAP-2	WFAP-1	WFAP-2	Small years	Large years
0.4 to 2.5	70	0	0	0.0%	0.0%	6.6	2.0
2.5 to 5.0	22	3	4	13.6%	18.2%	8.1	3.1
5.0 to 10.0	33	5	8	15.2%	24.2%	12.3	4.4
10.0 to 20.0	18	6	7	33.3%	38.9%	16.8	8.5
>20.0	20	11	11	55.0%	55.0%	56.2	82.0
All fires	163	25	30	15.3%	18.4%		
>2.5	93	25	30	26.9%	32.3%		

The burned areas are presented as buffered fire sizes because the process of adding a 1 km border to each fire boundary resulted in the merging of some of the individual fire events.

Table 2. Linear Relationship Between Area Burned as a Function of WFAP Active Fire Counts

		WFAP-1			WFAP-2			WFAP-M		
		Slope	R^2	*P*	Slope	R^2	*P*	Slope	R^2	*P*
East Canada		1002	0.74	<0.005	672	0.74	<0.005	1054	0.76	<0.001
West/Central Canada		564	0.84	<0.001	422	0.85	<0.001	564	0.84	<0.001
North Canada		518	0.63	<0.001	380	0.63	<0.001	575	0.57	<0.001
N. Canada (w/o Alaska)		507	0.97	<0.001	372	0.97	<0.001	572	0.97	<0.001
	Area burned (10^6 ha)									
1997	1.38	997	0.92	<0.001	650	0.92	<0.001	1098	0.85	<0.001
1998	4.69	535	0.91	<0.001	394	0.91	<0.001	565	0.91	<0.001
1999	2.09	497	0.67	<0.002	368	0.70	<0.001	682	0.75	<0.001
2000	0.99	737	0.48	<0.02	513	0.50	<0.02	746	0.45	<0.02
2001	0.7	1108	0.10	<0.31	753	0.22	<0.13	1185	0.15	<0.2
Overall		544	0.74	<0.001	445	0.74	<0.001	617	0.72	<0.001

The slope of the regression line represents the relative rate of detection of fires by the ATSR thermal IR channel, e.g., the area burned per active fire count.

The data in Table 2 show that except for 2001, significant linear correlations ($p < 0.02$) existed between area burned and WFAP fire count, with the efficiency of fire detection rising as annual area burned increased.

4. Discussion

[9] Factors influencing the detection rate of wildfires by thermal IR sensors include those related to the orbital and viewing geometry of the sensor, fire growth rates, fire intensity and size, and fire obscuration by clouds, smoke and atmospheric moisture [*Eva and Lambin*, 1998]. The potential number of pixels detected from a specific fire event (N) can be modeled as:

$$N = f(F_i,\ G_r) \tag{1}$$

where F_i is the imaging frequency, and G_r is the fire growth rate. The actual number of active fire counts (FC) detected from a fire event can be modeled as:

$$FC = f(N, O_r, D_r) \tag{2}$$

where O_r is the rate of fire obscuration by clouds and smoke, and D_r is the rate of fire detection. Equations (1) and (2) assume the burning area is much smaller than the pixel size of the instrument, which holds true for the 1 km resolution of the ATSR, but not for airborne and satellite systems with smaller pixel sizes.

[10] Since F_i is constant for the ATSR sensor, the results from this study suggest G_r, O_r, and/or D_r vary for the different years of this study. Growth patterns of boreal fires are determined by wind speed and direction. Area burned can be estimated as the area of an ellipse with a length, L, and breadth, B (area = $\pi \times L \times B$) [*Van Wagner*, 1969]. In satellite detection of fires, however, it is not the growth in burned area that is important, but the length of the active fire perimeter, which is calculated as the growth of the perimeter length or circumference of an ellipse [$\pi \times (L + B)$]; thus, the perimeter of a fire grows as a linear function of the rate of spread of the fire (Figure 3). Figure 4 shows that the weekly rate of growth in area burned in the North American boreal forest region varies as a function of seasonal fire activity, with higher area burned growth rates occurring during large fire years. Based on Figure 3, this suggests that the number of potential fire pixels should be lower for an individual fire event during the larger fire years.

[11] *Boles and Verbyla* [2000] showed the presence of clouds impeded viewing active fires with the AVHRR sensor. *Skinner et al.* [1999] concluded the annual area burned in the

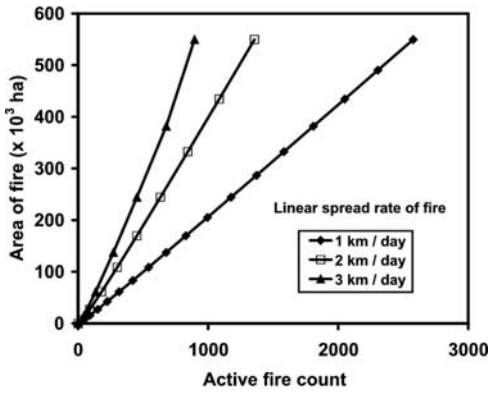

Figure 3. Theoretical relationship between area burned as a function cumulative number of active fire counts for three different spread rates (Sr) (1 km day-1: 211 ha/fire count; 2 km day-1: 397 ha/fire count; 3 km day-1: 582 ha/fire count). To estimate the spread rate of a fire, we assumed: (a) the fire started on day 0 and grew with 3 different spread rates; (b) the ratio of L and B are constant, with B = 0.6 L; and (c) the satellite imaged the fire once every three days.

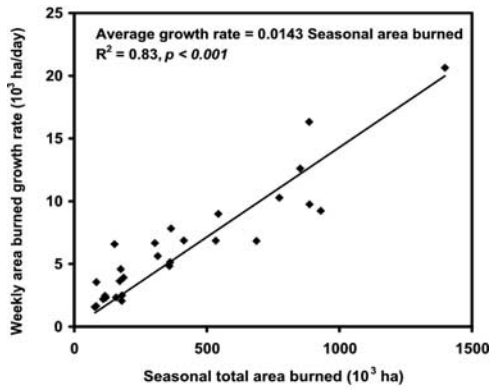

Figure 4. Weekly average area burned growth rate as a function of seasonal area burned for different provinces, territories, and states in the North American boreal forest region for the period of 1997 to 2002 based on daily and weekly area burned statistics from fire management agencies.

boreal forest region varies in response to shifts in the seasonal position of high-pressure ridges which controls the flow of moist, maritime air masses; thus, large fire years occur when high pressure ridges result in extended periods of low precipitation and cloud cover. Based on these observations, obscuration rates (O_r) should be lower during large fire years. In addition, the faster area burned growth rates during larger fire years (Figure 4) may be the result of more intense fires, increasing the probability of detection (D_r).

[12] In summary, we suggest the higher rates of detection during large fire years (Table 2) were the result of lower levels of cloud cover and higher intensity of fires, which increased the number of detections per individual fire event. This increase counter-balances the lower detection rates associated with higher spread rates that occur during high fire years (Figure 3).

5. Conclusions

[13] This study suggests using WFAP fire counts to assess burned area in the boreal forest region requires adjustments to account for variations in the relative detection rates between different regions and fire years. While the nighttime monitoring scheme used in the WFAP was intended to reduce false detections, it does not appear to be effective in higher latitude regions where the long summer daylight hours interfere with detection at the time of the satellite overpass.

[14] When data from Alaska were removed from the analyses, significant linear correlations existed between area burned and WFAP fire counts in different regions and for most years in the North American boreal forest. Variations in the slope of the regression line between regions and years show the assumption that the average rates of detection (D_r), obscuration (O_r) and fire spread rate (S_r) are constant between years is not valid. It appears that the sampling rate for ATSR may be related to level of annual fire activity, and that a correction can be made to the data to account for this bias.

[15] Many of the same climatic factors controlling fire activity in the boreal region also exist in other areas where significant biomass burning occurs. For example, in tropical regions of Asia, more fire activity occurs during ENSO events than during other years because of the extended periods of dry conditions [*Siegert et al.*, 2001]. One would expect cloud cover, fire intensity, and spread rate to vary in this region between low and high fire years as well, which in turn, would influence the overall rates of detection by thermal IR sensors. *Eva and Lambin* [1998] showed AVHRR active fire counts were proportional to area burned in Central Africa ($R^2 = 0.5$), but only after the data were aggregated to large (15 by 15 km) areas. While thermal IR sensors do indicate the occurrence of low and high fire years on a regional scale, scaling fire activity to area burned or trace gas emissions is not a simple linear transformation.

[16] **Acknowledgments.** The research presented in this paper was supported by NASA's Interdisciplinary Science Program through grants NAG5- 9440 (University of Maryland) and NAG5-9462 (California Institute of Technology).

References

Arino, O., M. Simon, I. Piccolini, and J. Rosaz, The ERS-2 ATSR-2 World Fire Atlas and the ERS-2 ATSR-2 World Burnt Surface Atlas Projects, in *8th ISPRS Conference on Physical Measurement & Signatures in Remote Sensing, Aussois, 8–12 Jan. 2001*, Aussois, 2001.

Bergamaschi, P., R. Hein, M. Heimann, and P. J. Crutzen, Inverse modeling of the global CO cycle - 1. Inversion of CO mixing ratios, *J. Geophys. Res.*, *105*, 1909–1927, 2000.

Boles, S. H., and D. B. Verbyla, Comparison of three AVHRR-based fire detection algorithms for interior Alaska, *Remote Sens. Environ.*, *72*, 1–16, 2000.

Dozier, J., A Method for satellite identification of surface-temperature fields of subpixel resolution, *Remote Sens. Environ.*, *11*, 221–229, 1981.

Duncan, B. N., R. V. Randall, A. C. Staudt, R. Yevich, and J. A. Logan, Interannual and seasonal variability of biomass burning emissions constrained by satellite observations, *J. Geophys. Res.*, *108*, ACH 1–1 to 1–22, 2003.

Dwyer, E., J.-M. Gregoire, and J.-P. Malingreau, A global analysis of vegetation fires using satellite images: Spatial and temporal dynamics, *Ambio*, *27*, 175–181, 1998.

Eva, H., and E. F. Lambin, Remote sensing of biomass burning in tropical regions: Sampling issues and multisensor approach, *Remote Sens. Env.*, *64*, 292–315, 1998.

FAO, Forest Fire Statistics, *Timber Bulletin*, *LII*, 1999.

Fuller, D. O., and M. Fulk, Burned area in Kalimantan, Indonesia mapped with NOAA AVHRR and Landsat Imagery, *Int. J. Remote Sens.*, *22*, 691–697, 2001.

Giglio, L., J. D. Kendall, and C. J. Tucker, Remote sensing of fires with the TRMM VIRS, *Int. J. Remote Sens.*, *21*, 203–207, 2000.

Goldammer, J. G., *Fire in Tropical Biota*, pp. 497, Springer-Verlag, New York, 1990.

Hao, W. M., and D. E. Ward, Methane production from global biomass burning, *J. Geophys. Res.*, *98*, 20,657–20,661, 1993.

Justice, C. O., L. Giglio, S. Korontzi, J. Owens, J. T. Morisette, D. Roy, J. Descloitres, S. Alleaume, F. Petitcolin, and Y. Kaufman, The MODIS fire products, *Remote Sens. Environ.*, *83*, 244–262, 2002.

Kasischke, E. S., and B. J. Stocks, *Fire, Climate Change, and Carbon Cycling in the Boreal Forest*, pp. 461, Springer-Verlag, New York, 2000.

Kasischke, E. S., D. Williams, and D. Barry, Analysis of the patterns of large fires in the boreal forest region of Alaska, *Int. J. Wild. Fire*, *11*, 131–144, 2002.

Lavoue, D., C. Liousse, H. Cachier, B. J. Stocks, and J. G. Goldammer, Modeling of carbonaceous particles emitted by boreal and temperate wildfires at northern latitudes, *J. Geophys. Res.*, *105*, 26,871–26,890, 2000.

Moreno, J. M., and W. C. Oechel, The Role of Fire in Mediterranean-Type Ecosystems, pp. 201, Springer-Verlag, New York, 1994.

Scholes, R. J., J. Kendall, and C. O. Justice, The quantity of biomass burned in southern Africa, *J. Geophys. Res.*, *101*, 23,667–23,676, 1996.

Schultz, M. G., On the use of ATSR fire count data to estimate the seasonal and interannual variability of vegetation fire emissions, *Atmosph. Chem. Physics*, *2*, 387–395, 2002.

Siegert, F., G. Ruecker, A. Hinrichs, and A. A. Hoffmann, Increased damage from fires in logged forests during droughts caused by El Nino, *Nature*, *414*, 437–440, 2001.

Skinner, W. R., B. J. Stocks, D. L. Martell, B. Bonsal, and A. Shabbar, The association between circulation anomalies in the mid- troposphere and area burned by wildland fire in Canada, *Theor. Appl. Climat.*, *63*, 89–105, 1999.

Stocks, B. J., J. A. Mason, J. B. Todd, E. M. Bosch, B. M. Wotton, B. D. Amiro, M. D. Flannigan, K. G. Hirsch, K. A. Logan, D. L. Martell, and W. R. Skinner, Large forest fires in Canada, 1959–1997, *J. Geophys. Res.*, *108*, 5-1 to 5-12, 2003.

Stroppiana, D., S. Pinnock, and J.-M. Gregoire, The Global Fire Product: Daily occurrence from April 1992 to December 1993 derived from NOAA AVHRR imagery, *Int. J. Remote Sens.*, *21*, 1279–1288, 2000.

van der Werf, G. R., J. T. Randerson, G. J. Collatz, and L. Giglio, Carbon emissions from fires in tropical and sub-tropical ecosystems, *Glob. Change Biol.*, *9*, 547–562, 2003.

Van Wagner, C. E., A simple fire-growth model, *Forest Chron.*, *45*, 103–104, 1969.

E. S. Kasischke and J. H. Hewson, 2181 LeFrak Hall, Department of Geography, University of Maryland, College Park, MD 20742, USA. (ekasisch@geog.umd.edu; jhewsons@glue.umd.edu)

B. Stocks, Canadian Forest Service, Sault Ste. Marie, Ontario P6A 2E5 Canada. (bstocks@nrcan.gc.can)

G. van der Werf, USDA-FAS, Code 923, NASA Goddard Space Flight Center, Greenbelt, MD 20771, USA. (guido@lptmailx@gsfc.nasa.gov)

J. Randerson, Divisions of Geological and Planetary Sciences and Engineering and Applied Science, California Institute of Technology, Mail Stop 100-23, Pasadena, CA 91125, USA. (jimr@gps.caltech.edu)